

The lives and deaths of positrons in the interstellar medium

N. Guessoum¹, P. Jean², and W. Gillard²

¹ American University of Sharjah, College of Arts & Sciences, Physics Department, PO Box 26666, Sharjah, UAE

² CESR, CNRS/UPS, B.P. 4346, 31028 Toulouse Cedex 4, France

Received ; accepted

Abstract.

We reexamine in detail the various processes undergone by positrons in the interstellar medium (ISM) from their birth to their annihilation using the most recent results of positron interaction cross sections with atomic and molecular hydrogen, as well as helium. The positrons' lives are divided into two phases: the “in-flight” phase (between ≈ 1 MeV and tens of eV) and the thermal phase. The first phase is treated with a Monte Carlo simulation that allows us to determine the fraction of positrons that form positronium and annihilate as well as the characteristics of the annihilation emission as a function of the medium conditions. The second phase is treated with a binary reaction rate approach, with cross sections adopted from experimental measurement or theoretical calculations. An extensive search and update of the knowledge of positron processes was thus undertaken. New reaction rates and line widths have been obtained.

We investigate the treatment of the complicated interactions between positrons and interstellar dust grains. Fully relevant data were not always available, but we were nonetheless able to reach satisfactory understanding of positron annihilation on grains, both qualitatively and quantitatively. All factors of the problem have been considered, including the grain size distribution and composition, the electric charge of the grains, the backscattering, positronium formation and ejection from the grain, the pick-off annihilation inside them and the partial destruction of dust in the hot regions of the ISM. New reaction rates and widths of the line resulting from the annihilation inside and outside of the grain have been obtained. The final results of our calculations (reaction rates and spectra) showed that dust is only important in the hot phase of the ISM, where it dominates all other processes.

Combining the new calculations, we have constructed annihilation spectra for each phase of the ISM, considering various grain contents, as well as an overall combined spectrum for the ISM as a whole.

Key words. Gamma rays: theory – Line: formation, profile – ISM: general

1. Introduction

Positrons are produced at tremendous rates in the Galaxy. This has been firmly established by a long series of balloon and satellite detections of the positrons' landmark signature, the gamma-ray line at 511 keV produced in their annihilation with electrons. A rate of $\approx 10^{43} e^+/s$ is usually inferred from such detections (Purcell et al. 1997, Milne et al. 2000). Surprisingly, despite three decades of (indirect) detections of positrons, the origin and galactic distribution of these huge amounts of antiparticles is still puzzling astrophysicists. There are several major reasons for this problem: 1) our understanding of the positron production processes in astrophysical media is plagued by significant uncertainties; 2) the galactic map of the 511 keV annihilation line, which is supposed to lead us to the positrons, has yet to be determined with any reasonable accuracy; 3)

the physics of the annihilation processes, which have until now been believed to be well understood, may need to be improved to a certain extent; 4) our lack of knowledge of the extent of diffusion/propagation of positrons between their production sites and their annihilation places.

In nature, positrons can be produced by one of the following main processes: a) β^+ decay of radioactive nuclei; b) π^+ decay into μ^+ , which decays and gives off a positron; c) pair (electron-positron) production through photon-photon interactions; d) pair production by the interaction of an electron with a strong magnetic field. All these processes can be found in astrophysical settings, provided that the physical conditions for them are fulfilled. For example, the first process (the β^+ decay of a radioactive nucleus) is widespread in the explosive and/or hydrostatic nucleosynthesis environments of novae, supernovae, Wolf-Rayet and Asymptotic Giant Branch stars. The sec-

ond process ($\pi^+ \rightarrow \mu^+ \rightarrow e^+$) takes place where the pion is produced in collisions of highly energetic (more than ≈ 200 MeV) cosmic rays with interstellar material (mostly protons). The third process (photon-photon pair production) requires photons of high energies and is known to occur in the environment of luminous compact objects (black hole candidates, micro-quasars, active galactic nuclei, etc.). The fourth process requires intense magnetic fields and is rather common in the environments of pulsars/neutron stars.

On the scale of the whole Galaxy, as we are interested in here, the main positron generators are, in order of decreasing importance: supernovae (SNe), novae (Ne), compact objects (microquasars, pulsars, etc.), cosmic rays and possibly gamma ray bursts. However, substantial uncertainties over the specific factors involved in each case have made the precise identification of the positron sources very difficult. For instance, for the main candidates for galactic positrons (supernovae), depending on their type, the specific positron production process and the escape fraction from the expanding shell into the interstellar medium (ISM), the amount of positrons contributed by supernovae may vary significantly.

The issue of the origin of positrons responsible for the observed annihilation in the Galaxy will be investigated in another work, in relation to the new 511 keV map(s) obtained by INTEGRAL/SPI (Knodlseder et al. 2005). For a recent review of some of the issues pertaining to this topic, see the paper by Paul (2004) or Jean et al. (2004). We will address here only the physics of the annihilation as it leads to the spectra observed by high energy-resolution instruments.

Since the discovery of the 511 keV annihilation radiation emanating from the Galactic center in 1970 (Johnson, Harnden and Haymes 1972), interest in this radiation, from the observational viewpoint as well as from the theoretical stance, has been very high.

On the observational side, dozens of balloon and, more recently, satellite missions have been conducted over the past 2 or 3 decades. We will cite only high energy-resolution (germanium) instruments that allowed for the extraction of a detailed line spectrum, because the physics of the annihilation produces a spectrum that can only be compared to one obtained by such instruments. In 1977 the Ge-detector (high energy resolution) balloon mission (Leventhal, MacCallum and Stang 1978), established the electron-positron annihilation nature of the radiation by accurately measuring the line centroid energy at 511 keV. The Gamma-Ray Imaging Spectrometer (GRIS) balloon missions (Gehrels et al., 1991; Leventhal et al. 1993) firmly established the narrow width of the line (FWHM less than about 3 keV) and separated the extended, diffuse emission in the interstellar medium (ISM) from that of the Galactic center region. The HEXAGONE balloon-borne spectrometer mission (Chapuis et al., 1991; Drououchoux et al. 1993) also detected a narrow line (FWHM less than about 3 keV). The Transient Gamma-Ray Spectrometer (TGRS), onboard the WIND satellite, rather strongly disproved the

two-component, time-variability (of the Galactic Center emission) paradigm (Teegarden et al., 1996; Harris et al. 1998; Harris 2000) and showed an even narrower line (FWHM ≈ 1.8 keV). The most recent analysis of the data from the on-going INTEGRAL/SPI detection of the annihilation line shows the line to have a width of ≈ 2.3 keV (Knodlseder et al. 2005).

In parallel, theoretical modeling and data analyses of the emission have proceeded in an attempt to understand both the physical processes behind the emission and the physical conditions prevailing in the regions where the annihilation is taking place.

Detailed theoretical investigations of the annihilation processes behind the observed radiation go back to Crannell et al. (1976) who, while interested in the line produced specifically in solar flares, investigated most of the processes involved in electron-positron interactions. Other researchers, i.e. Steigman (1968), Stecker (1969) and Leventhal (1973) had pointed out the importance of the Positronium in astrophysical settings. Positronium (Ps) is the bound state of a positron with an electron, and depending on whether the two have parallel or anti-parallel spins, this “atom” will be in the long-lifetime ($t = 140$ ns) ortho-Ps state or the short-lifetime ($t = 0.125$ ns) para-Ps state. The latter decays into 2 photons of 511 keV (plus or minus some small amount of energy corresponding to the relative momenta of the bound particles), while the former (ortho-Ps) state decays into 3 photons of energies totaling 1022 keV. The distribution of photon energies resulting from the decay of ortho-Ps was first calculated by Ore & Powell (1949) and more recently by Adkins (1983).

Subsequent work on the positron processes focused on the conditions of the interstellar medium. Bussard, Ramaty and Drachman (1979 – hereafter BRD79) calculated the rates of the various processes undergone by low-energy positrons and obtained the resulting annihilation spectrum; Ramaty & Meszaros (1981) considered the processes and the resulting radiation in the conditions of a relativistic, hot (high-temperature) plasma. Zurek (1985) emphasized the role of dust grains and showed their potentially important modification of the annihilation spectrum, especially in the hot/warm/ionized phases of the ISM. Guessoum, Ramaty and Lingenfelter (1991) reconsidered the problem in light of earlier developments (new calculations of reaction rates by Gould 1989, recent observational data, more precise treatment of dust grains, etc.), performed detailed theoretical spectroscopy of the annihilation line, and produced spectra for various conditions of the ISM; one of the ideas emphasized in that work was that the FWHM value was not an accurate descriptor of the line, as the line cannot always be simply represented or fitted by a Gaussian function. Guessoum, Ramaty and Skibo (1997) updated the knowledge of positron processes (reaction rates and line widths), adding molecular hydrogen and helium. Most recently, Dermer & Murphy (2001) reviewed the positron production and annihilation mechanisms, dealing with both the sources of positrons and the line profile depending on the annihilation environment.

Positron annihilation models for astrophysical settings also rely heavily on many laboratory measurements and theoretical calculations of positron interactions with atoms and molecules. We mention the pioneering work of: Bhatia, Drachman and Temkin (1977) for early theoretical calculations of annihilation in positron-hydrogen collisions; Brown et al. (1984), Brown, Leventhal and Mills (1986), Brown & Leventhal (1986) for measurements of line widths and Positronium formation fractions in gases (H_2 , He) relevant to the ISM conditions; see Charlton & Humberston (2001) for a general review of positron work in gases (particularly H , H_2 , He), Puska & Nieminen (1994) for the theory of positrons in solids and on solid surfaces, and the body of work by Iwata, Surko and collaborators (Iwata et al. 1996, Iwata et al. 1997, Iwata et al. 2000) on laboratory measurements of cross sections and annihilation line widths of positrons colliding with atoms and molecules (up to and including large complex alcohol and/or aromatic molecules, some of which may exist in galactic molecular clouds). We would draw attention to the significant amount of relevant “non-astrophysical” work currently being performed by atomic and condensed matter researchers in positron physics¹.

In order to determine the overall spectrum of the line produced by the galactic positrons, one must consider a model of the ISM, i.e. distributions and characteristics (temperature, ionization, etc.) of the gas (H , H_2 , He) and dust. Guessoum, Ramaty and Lingenfelter (1991) based their work on the model of McKee & Ostriker (1977); Gillard (pers. comm.) use the models of Ferriere (1998a, 1998b, 2001), deeming them more detailed and more conveniently described by analytical expressions.

Taking all the above physical information (processes, cross sections, line widths, gas distributions, etc.) into account, one can attempt to reproduce the observational data (from GRIS, HEXAGONE, TGRS, INTEGRAL/SPI) and infer useful knowledge about the environment where the annihilation is predominantly taking place. This kind of approach was adopted by Wallyn et al. (1993) for the HEXAGONE data and by Guessoum et al. (2004) for the SPI and the TGRS data.

The latest such analysis (Guessoum et al. 2004) partly led us to revisit the subject of positron processes and annihilation. Analysis of the SPI data (for which the FWHM was then (2.67 ± 0.33) keV - Lonjou et al. 2004), unlike that of TGRS (for which the FWHM was (1.8 ± 0.5) keV - Harris et al. 1998) tended to imply a very large amount (or reaction rate) of dust grains, simply because the interaction of positrons with grains resulted (in the treatments done until now) in a line made up of two Gaussians, one

¹ See the work by the groups at University of California, San Diego (<http://physics.ucsd.edu/research/surkogroup/positron/>), Surko et al. (2000); the groups at Martin-Luther-University Halle (<http://positron.physik.uni-halle.de/>), at University of Michigan (<http://positrons.physics.lsa.umich.edu/>); and others.

with $\Gamma = 2.5$ keV and one with $\Gamma = 1.8$ keV. Similarly, the cross section for positron-hydrogen charge exchange had been known to be extremely important, because this reaction dominates all other processes in the cold phases of the ISM, and because it leads to both a wide line (6.4 keV in the old treatments) and a large Ps fraction (f_1 , the fraction of the positrons that annihilate via Positronium formation). We thus realized that a detailed and refined treatment of positron processes was needed before one can attempt to analyze the high-quality data and draw astrophysical conclusions from it.

In the next section, we review the processes that take place “in flight”, i.e. before the positrons thermalize with the medium of the given ISM phase; this applies for positron energies between ≈ 1 MeV (their kinetic energies when they come out of beta decay) and a few tens of eV, when Positronium formation through charge exchange starts to occur. This regime includes Coulomb energy losses (with free electrons), excitation and ionization of atoms (H , H_2 , He), and Ps formation by charge exchange with H , H_2 and He. We review the cross sections for all the relevant processes and perform a Monte Carlo simulation to determine the width of the line produced in this regime. This is done with utmost care because of the importance of the charge exchange process as explained above. In section 3, we review the positron processes after thermalization; these comprise: charge exchange with H , H_2 , He, direct annihilation with bound electrons, direct annihilation with free electrons and radiative combination (with free electrons). We discuss the dust grains and the processes that positrons undergo with them. We also present up-to-date line widths for all processes. In section 4, we use the knowledge compiled and presented here to obtain annihilation spectra in standard ISM situations. In the final section, we summarize the most important new information and discuss the application of this revision to the 511 keV SPI data analysis that we intend to perform.

2. In-flight processes

When, after being slowed down by Coulomb collisions in the ISM, the positron has an energy less than a few tens of eV, it starts to pick up an electron from an atom or a molecule by charge exchange, thus forming a positronium. This process is endoenergetic; it can happen as long as the kinetic energy of the positron is above the charge exchange threshold energy of Ps formation with the given atom or the molecule. We calculate the probability for such an event to occur using the Monte Carlo method, similarly to the method presented in BRD79. In the following sections we present the cross sections we used for the calculation and the results of the simulation for positrons in atomic and molecular hydrogen and helium.

2.1. Energy losses and cross-sections

In a partially ionized medium, the positron loses its energy by collisions with electrons and by interaction with plasma

Table 1. Energy threshold of reactions induced by positrons.

Process	Threshold (eV)
$e^+ + H \rightarrow Ps + H^+$	6.8
$e^+ + H \rightarrow e^+ + e^- + H^+$	13.6
$e^+ + H \rightarrow e^+ + H^*$	10.2
$e^+ + H \rightarrow e^+ + H^{**}$	12.1
$e^+ + He \rightarrow Ps + He^+$	17.8
$e^+ + He \rightarrow e^+ + e^- + He^+$	24.6
$e^+ + He \rightarrow e^+ + He^*$	21.2
$e^+ + H_2 \rightarrow Ps + H_2^+$	8.6
$e^+ + H_2 \rightarrow e^+ + e^- + H_2^+$	15.4
$e^+ + H_2 \rightarrow e^+ + H_2^*$	12.0

waves, excitation and ionization of atoms and molecules. The energy loss in the plasma is a continuous process. Its rate, which depends on the energy of the positron, the electron temperature and density in the plasma, is given by Book and Ali (1975). The other processes require a collision with an individual atom or molecule. In this case the amount of the energy lost by the positron depends on the positron energy and on the type of collision: excitation or ionization. The thresholds for all these processes are presented in Table 1. Figures 1a, 1b & 1c show the cross sections we used for for excitation, ionization and charge exchange in H, H₂ and He respectively.

2.1.1. Hydrogen

The various cross section measurements for positron-impact ionization of H we have found in the literature (Jones et al. 1993; Hofmann et al. 1997 and Kara 1999) are in agreement, except those of Spicher et al. (1990) which are thought to have a systematic normalisation error (Charlton and Humberston 2001 - hereafter CH2001). On the theoretical side, the results of calculations by Janev & Solov'ev (1998) fit the previous measurements below 40 eV, whereas those of Ratnavelu (1991) are in good accord with the data above 30 eV but slightly overestimate the cross-section in the 150-300 eV range.

We have thus reconstructed the cross section dependence on the positron kinetic energy by using the calculations of Janev & Solov'ev (1998) below 40 eV and averages of the experimental data above this value. The energy loss by positrons in such a collision has been approximated by BRD79 to be distributed as a Gaussian with a mean of one-fourth of the binding energy and a standard deviation of ≈ 2 eV. We adopt this approximation, which was inspired by the calculations by Omidvar (1965) of the ejected electron velocities in electron-hydrogen ionization collision.

Concerning the positron-induced excitation of H we used the calculated cross sections of Walters (1988) and Kernoghan et al. (1996) for 1s-2s and 1s-2p excitations. The cross section for excitation of higher energy levels is taken from Fig. 3 of Stein et al. (1998). The latter has

been deduced by subtracting the elastic, ionization, 1s-2s and 1s-2p excitation and Ps formation cross sections calculated by Kernoghan et al. (1996) from their total calculated cross section. The positron energy lost in an excitation to the 2s or 2p levels of H is ≈ 10.2 eV. We assume the energy loss in excitation of the highest levels to be identical to the one for the n=3 level (12.1 eV).

Among the recent measurements of Ps formation cross sections (Sperber et al. 1992, Zhou et al. 1997, Kara et al. 1999), the results of Sperber et al. (1992), which were the first to be performed, differ significantly (a factor of 4/3) from the others and are thought to be incorrect (Hoffman et al. 1997). Ps formation cross sections calculated by Kernoghan et al. (1996) are in good accord with the experimental results of Zhou et al. (1997) and Kara et al. (1999). We thus use this calculation's results in modelling the cross section. Since the excitation and ionization processes dominate above 100 eV, measurements of the Ps formation cross section are subject to large uncertainties. For the same reasons, the extrapolation of the charge exchange cross section by a power law or by an exponential cut does not affect the results of the fraction of Ps formation in-flight significantly.

2.1.2. Helium

Experiments for the measurement of the single ionization of helium by positron impact (Fromme et al. 1986; Knudsen et al. 1990; Jacobsen et al. 1995; Moxom, Ashley & Laricchia 1996) yield general agreement, except for the results of Fromme et al. (1986) which slightly overestimate the cross section below 50 eV and underestimate it (by $\approx 12\%$) in the 100-200 eV range. The calculation for positron kinetic energies below 150 eV made by Campbell et al. (1998) fits the data quite well (see also CH2001 p 241). We use this theoretical result for energies less than 150 eV and the average of the measurements above this value. The energy distribution of the ejected electron is taken from Goruganthu et al. (1985), who calculated the single differential cross section of secondary electron production for electron-impact ionization in helium. These distributions can be approximated by an exponential law with an energy scale of ≈ 18.5 eV. We neglected the He double ionization by a positron since its cross section is $\approx 3 \times 10^{-3}$ lower than that for single ionization (Charlton et al. 1988, CH2001).

The cross section for the excitation of He by positrons is not well determined, either by measurements or by calculations. Chapuis et al. (1994) deduced it from the difference between the total cross section and those of the charge exchange and ionization cross sections. However, the excitation cross-section for positron-He scattering evaluated with this method overestimates by a factor of ≈ 4 the experimental measurements (Coleman et al. 1982; Mori & Suoeka 1994) and theoretical calculations (Parcell et al. 1987; Hewitt, Noble & Bransden 1992; Ficocelli Varrachio & Parcell 1992; Campbell et al. 1998; see also

Fig. 5.4 of CH2001). We used the cross section curve of Chapuis et al. (1994) scaled to fit the most recent experimental results of Mori & Suoeka (1994).

While the measurements of the cross section for positronium formation in positron collisions with helium (Fornari, Diana & Coleman 1983; Diana et al. 1986; Fromme et al. 1986; Moxom et al. 1993; Overton et al. 1993) are in good agreement below ≈ 80 eV, large discrepancies occur above this value. These discrepancies may be due to experimental errors (CH2001), and the most recent results of Overton et al. (1993), which are lower than the other measurements above 80 eV, are in better accord with theoretical calculations of McAlinden & Walters (1992) and Campbell et al. (1998). We have used the results of the latter authors to model the cross section for charge exchange in helium.

2.1.3. Molecular hydrogen

The four cross section measurements by Fromme et al. (1988), Knudsen et al. (1990), Jacobsen et al. (1995) and Moxom et al. (1996) of the positron-impact single ionization of molecular hydrogen provide very different results for energies less than 200 eV (see also CH2001). The latest results of Moxom et al. (1996) seem more appropriate since they are not far from the results of Fromme et al. (1988) and Knudsen et al. (1990).

However, data of Jacobsen et al. (1995), which underestimate the results of previous experiments by $\approx 40\%$ at 80 eV, are the closest to the theoretical evaluations performed by Chen, Chen & Kuang (1992). So by choosing to use the cross section of Moxom et al. (1996), we ran the risk of making a systematic error in the calculation of the fraction of positronium formation in flight in molecular hydrogen. But, as presented in the next section, the results of this assumption provide a fraction in agreement with measurements of Brown & Leventhal (1986).

There are few measurements and studies on the energy distribution of the ejected electrons in ionisation collision of H_2 by positrons. Köver & Laricchia (1998), Berakdar (1998) and Köver, Paludan & Laricchia (2002) provide such a distribution, but only for forward electrons and specific positron energies. As for helium we approximate the distribution of the ejected electrons by an exponential law. According to the few existing measurements, the energy scale of this distribution is approximately 15 eV. Since the cross section for the dissociative ionization of molecular hydrogen by electrons contributes only to 6% of the ionization cross section (Rapp, Englander-Golden & Briglia 1965), we neglect this process in the simulation.

Measurements of the charge exchange cross section in molecular hydrogen are mostly in agreement (Fornari et al. 1983; Diana et al. 1986; Fromme et al. 1988; Zhou et al. 1997 – see also Kwan et al. 1998). However, the Fromme et al. (1988) results are above the upper limit derived by Zhou et al. (1997) for energies less than 10 eV. Therefore we have used the cross section measured by Fornari et al.

(1983) and Diana et al. (1986) for the low ($E < 100$ eV) and high ($E > 100$ eV) energies, respectively. It should be noted that the cross section derived by BRD79 fits the data of Fornari et al. (1983) quite well in the 15 – 50 eV range.

Very little is known from either theory or experiment concerning the excitation of molecules by positrons. We thus estimate the excitation cross section of positrons colliding with molecular hydrogen by subtracting the charge exchange, ionization and elastic cross sections from the total cross section, which has been measured by Hoffman et al. (1982). The elastic cross section was evaluated by Wallyn et al. (1994).

2.2. Positronium formation in flight

We simulate the interactions of positrons with atoms and molecules by Monte-Carlo methods on the basis of the cross sections and energy loss mechanisms presented previously. For any value of the positron's kinetic energy (that is at any stage of the simulation), the interaction process is chosen randomly according to the values of the cross sections of all the possible processes. The particular interaction then specifies the energy lost at that stage. The positron is “dropped” either when it forms a positronium or when its kinetic energy falls below the threshold of charge exchange; in the latter case, the positron is assumed to start thermalizing with the ambient medium.

The fraction f_1 of positrons forming a positronium in flight is then obtained simply by counting the number of positrons undergoing a charge exchange. When such a process occurs, the kinetic energy value of the positronium (i.e. the kinetic energy of the positron minus the energy required to form the positronium) is stored. The set of kinetic energies obtained from the simulation is then used to calculate the spectral shape of the annihilation emission by accounting for the Doppler broadening due to the motion of the positronium. The shapes of the annihilation line differ somewhat from a simple Gaussian, but we parametrize them with FWHMs by fitting Gaussian functions to the spectra (see section 3.2). We also record the time spent by positrons to slow down and reach the charge exchange threshold or form a positronium. The resulting mean duration deduced from a large number of positrons allows us to calculate the slowing down time of positrons before thermalization.

We tested our Monte Carlo simulation by reproducing the results obtained by BRD79 (see Figure 2). They calculated the fraction of positrons undergoing charge exchange with atomic hydrogen before thermalization as a function of the ionization fraction. Similarly our calculation has been performed for two cases of media characterized by their electron density and temperature. The first is representative of a warm component of the ISM ($T \sim 8000$ K) and the second of solar flares ($T \sim 10^6$ K).

Values of f_1 for a totally neutral medium are summarized in Table 2 where they are compared with results of previous measurements (Brown & Leventhal 1984, 1986)

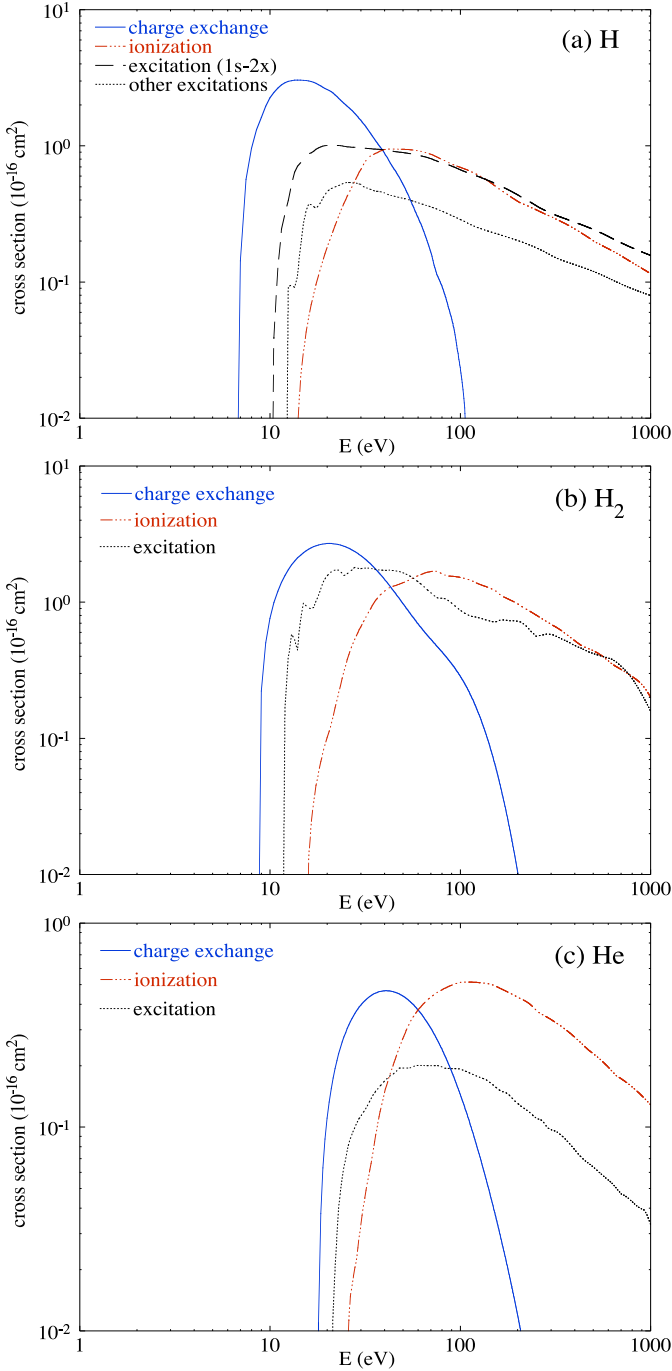


Fig. 1. Cross sections for positronium formation, ionization and excitation in positron collision with (a) atomic hydrogen, (b) molecular hydrogen and (c) helium as a function of the kinetic energy.

and calculations (BRD79; Wallyn et al. 1994; Chapuis et al. 1994).

3. Processes after thermalization

After they have lost the bulk of their energies during the “in-flight” phase, the positrons thermalize with the ambient medium and undergo a series of processes leading

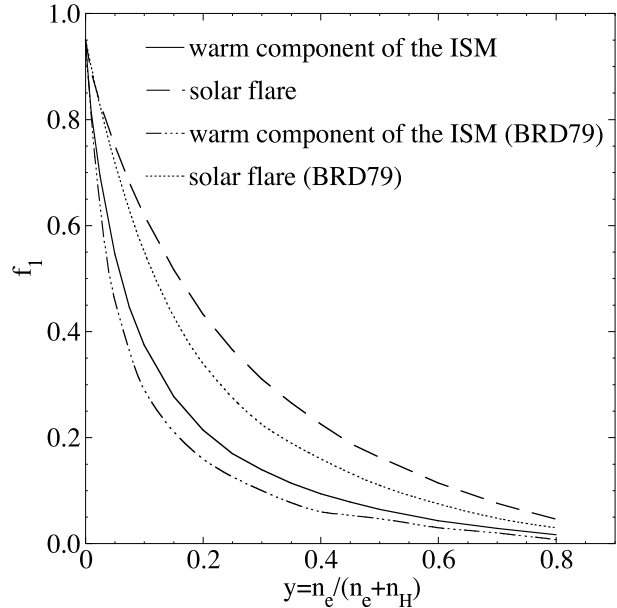


Fig. 2. Fraction of positrons forming positronium in flight (f_1) by charge exchange with atomic hydrogen as a function of the ionization fraction (y) in a warm component of the interstellar medium (electron density: $n_e = 0.1 \text{ cm}^{-3}$, electron temperature: $T_e = 8000 \text{ K}$) and in solar flare ($n_e = 5 \times 10^{13} \text{ cm}^{-3}$, $T_e = 1.16 \times 10^4 \text{ K}$). The results presented in Fig. 2 of BRD79 are shown for comparison.

Table 2. Fraction (in %) of positrons forming positronium in flight, in a completely neutral medium.

References	H	H_2	He
BRD79	95	93	—
Brown & Leventhal	—	89.7 ± 0.3	80.7 ± 0.5
Wallyn et al. 1994	98	90	—
Chapuis et al. 1994	—	—	78
This paper	95.5	89.6	81.7

to their annihilation, either directly or via positronium formation.

3.1. Reaction rates for positron processes

In thermal conditions, the reaction rate for non-relativistic binary collisions is easy to calculate; we use the usual $\langle \sigma v \rangle$ formula, where the averaging is done over the interacting particles’ (Maxwellian) energy distributions:

$$R = \langle \sigma v \rangle = \int_{E_T}^{\infty} \frac{2}{\sqrt{\pi}} \frac{\sqrt{E}}{(kT)^{3/2}} e^{-E/kT} \sigma(E) v dE. \quad (1)$$

3.1.1. Charge exchange with H, H_2 , He

The cross sections for these reactions were discussed in the previous section. The calculated rate is shown in Figure 3 along with the rates of the other processes. These rates

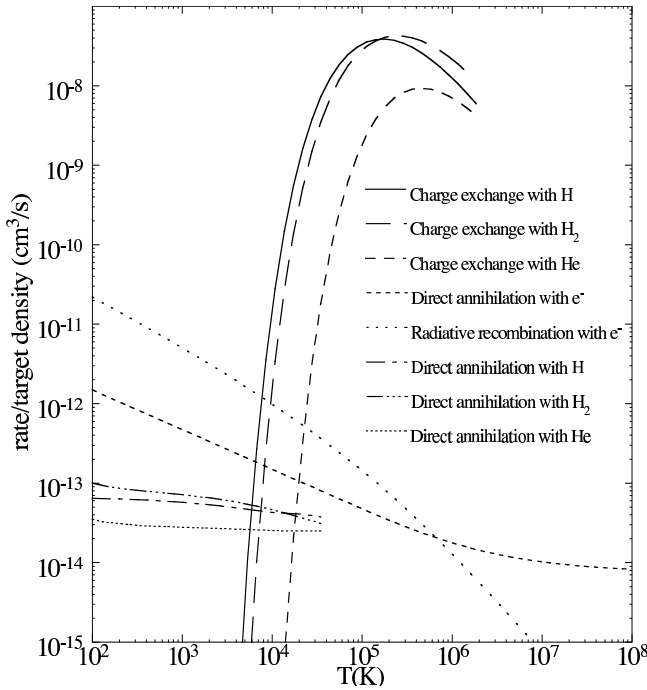


Fig. 3. Positron reaction rates as a function of temperature.

are significant only above a few times 10^4 K, when the high-energy tail of the Maxwellian distribution is above the threshold of Ps formation. Also, although few atoms remain neutral at such a high temperatures, we present the charge exchange rate up to 2×10^6 K.

3.1.2. Radiative combination (with free electrons)

The cross section for this process ($e^+ + e^- \rightarrow Ps + \gamma$) is so small (10^{-20} cm^2 at 1 eV and decreasing fast at higher energies) that it cannot be measured in the laboratory. We must thus rely on theoretical calculations. Various attempts and approaches have been made over the past several decades, going back to 1930, the most recent and accurate of which is that of Gould (1989), who obtained the reaction rate for both the ground state and the first excited state of Ps directly from first principles. The earlier calculation of Crannell et al. (1976) used the similarity between this process and the radiative recombination of hydrogen ($e^- + p \rightarrow H + \gamma$) for which the cross section was already known.

3.1.3. Direct annihilation with free electrons

This process ($e^+ + e^- \rightarrow \gamma + \gamma$) has a very small cross section (about an order of magnitude less than that of radiative combination at temperature less than 10^5 K – Heitler 1954; Crannell et al. 1976; BRD79). It is therefore only relevant in the hot phase of the ISM and can be ignored in all other conditions, as can be seen in Figure 3.

3.1.4. Direct annihilation with bound electrons

This process ($e^+ + H \rightarrow p + \gamma + \gamma$, or e^+ on H_2 or on He) has the lowest cross section of all the positron processes, more than an order of magnitude less than the second slowest process, direct annihilation with free electrons, and more than two orders of magnitude weaker than radiative combination. Direct annihilation with bound electrons applies only at the lowest temperatures (less than a few thousand degrees) where charge exchange does not proceed because the positrons then do not have the threshold energy needed and there are no free electrons for the other two processes – radiative combination and direct annihilation with free electrons – to take place. Due to the weakness of its cross section, this process cannot be investigated in the laboratory, and again one must rely on theoretical calculations. The work of Bhatia, Drachman and Temkin (1977) has not been corrected or updated by any later works, so we still use the rate they obtained for direct annihilation with H. For He and H_2 the method is similar, except that we calculated the cross section using estimates of the dependence of Z_{eff} , the effective charge², on the kinetic energy from Campeanu & Humberston (1977) and Armour, Baker & Plummer (1990), respectively.

The measured Z_{eff} in H_2 at room temperature is $\approx 45\%$ larger than the theoretical evaluation (CH2001). This may turn out to be a source of systematic error in the annihilation rate we will be using.

3.2. Line widths

The widths of the annihilation line resulting from charge exchange in flight with H, H_2 , and He have been calculated as a result of the Monte Carlo simulation we presented in the previous section. We have found 5.8 keV, 6.4 keV and 7.4 keV for H, H_2 and He respectively in a neutral medium. These widths are in quite good agreement with previous measurements and calculations (BRD79, Brown & Leventhal 1984, Brown & Leventhal 1986). The width of the 511 keV line does not vary with the ionisation fraction of the ambient medium although its shape is slightly “flattened” (the top of the spectral distribution is less peaked). This flattening is due to the loss of low energy positrons which are quickly slowed down below the Ps threshold by way of Coulomb collisions with electrons.

The widths of the annihilation line resulting from the direct annihilation with H, H_2 , and He have all been measured experimentally: Brown & Leventhal (1986) obtained 1.56 keV for H; and Iwata, Greaves, and Surko (1997) obtained 1.71 keV and 2.50 keV for H_2 and He, respectively. These widths depend very weakly on the temperature in our range of interest.

The widths of both the radiative combination and direct annihilation with free electrons were calculated by Crannell et al. (1976) using a simple argument of thermal

² The effective charge Z_{eff} is defined such that the annihilation rate per target density is $R = \sigma v = Z_{eff} c \pi r_e^2$, with r_e the classical electron radius.

broadening due to the motion of the center of mass of the e^+e^- pair; this calculation gives the same following simple expression for both widths: $\Gamma_{rc,dae} = 1.1 T_4^{1/2}$ keV, where T_4 is the temperature in units of 10^4 K.

3.3. Grains and positron processes

The importance of positron capture and annihilation on interstellar dust grains was first pointed out by Zurek (1985), who estimated the rate for the process and concluded that dust can play a crucial role in the warm ionized phase of the ISM, leading to drastic modifications of the Ps formation fraction depending on the value of the cross section of the positron capture on the dust grains. Guessoum, Ramaty and Lingenfelter (1991) added spectral considerations to the positron-dust process but kept a simplified picture of the dust and showed that unless the abundance of dust in the annihilation regions is increased many times compared to “normal” quantities, grains change the spectrum of the line mostly in the hot phase. Astrophysical knowledge of grains has since increased considerably (see the reviews by Draine 2003, 2004, Li 2004, and Krugel 2003) and although a huge body of work exists on positron interactions with solids and solid surfaces (Niemenen & Oliva 1980; Huttunen et al. 1990; Dannefaer et al. 1996; Dupasquier & Mills 1995; Puska & Niemenen 1994; Weiss et al. 1994; Suzuki et al. 2003; Mills et al. 1989; Mokrushin et al. 2003; Pi et al. 2003; Weber & Lynn 2000), experiments dealing with positrons and dust like materials remain scarce. We here summarize our best understanding of the relevant information we have collected on dust grains in our context.

The total amount of dust in the Galaxy is estimated at $3 \times 10^7 M_\odot$, which represents 0.6 % of the total mass of gas (Krugel 2003), although Ferriere (2003) indicates that there is a large uncertainty on this fraction, which could range from 0.5 to 1 %. The abundance of dust grains is found to correlate approximately with hydrogen, particularly in the cold and neutral phases; there is also some evidence (Herter et al. 1989; Krugel 2003) for partial dust destruction in the HII regions.

Several species of dust (composition, size) exist in the ISM. Dust is often divided into 3 categories as follows:

- Large grains, of radii ranging between 20 nm and 0.3 μm , made of either silicate particles (Mg_2SiO_4 or Fe_2SiO_4) or amorphous carbon;
- Very small grains, of radii ranging between 1 nm and 10 nm, made mostly of graphite, and representing about 10 % of the amorphous carbons;
- PAH (polycyclic aromatic hydrocarbons), which are big molecules and make up 3 to 6 % of the large grains (in abundance).

We have ignored the PAHs in the present treatment due to their negligible contribution; in fact, we have found that the “very small grains” can be neglected as well, as their abundance and small sizes (small geomet-

ric cross sections) give extremely low positron capture rates.

Grain sizes follow a power-law distribution: $dn_{gr} \propto a^{-3/2}da$, where a is the radius of the grain, which ranges between 3×10^{-6} cm and 2.4×10^{-5} cm for the large carbonaceous grains and between 1.5×10^{-6} cm and 1.2×10^{-5} cm for the large silicate grains (Krugel 2003). Other distributions and grain size ranges that distinguish between grain types have also been proposed (Weingartner & Draine 2001; Li & Draine 2001), but we will adopt the simple unified expression of Krugel (2003). The distributions and grain size ranges given by Weingartner & Draine (2001) or Li & Draine (2001) lead to reaction rates that are several times higher than those we obtain with the “conservative” values of Krugel (2003). This factor (the sizes and distribution law of the grains) is the fundamental uncertainty in the determination of the reaction rate of positron interaction with the dust. Secondary factors include the amount of dust in the ISM (as stated previously) and the electric charge of the grains in the cold phase. We have combined these uncertainties into one parameter, denoted by x_{gr} (similar to that of Guessoum, Ramaty and Lingenfelter 1991), where $x_{gr} = 1$ represents our “standard” rate, obtained on the basis of the Krugel (2003) parametrization of dust; $x_{gr} = 0$ represents a total absence of dust in a given region; $x_{gr} > 1$ represents an overabundance of dust and/or grain characteristics (sizes and composition) that are especially favorable for positron capture. We emphasize however, that these factors do not affect our conclusions, namely that the reaction rates for positron capture on dust are, even in the most extreme assumptions, negligible compared to other processes in all but the warm-ionized and hot ISM phase: in the latter environment the dust dominates all other processes under all assumptions, and in the other case the dust becomes comparable or dominant only when the grain capture rate (or equivalently x_{gr}) is increased by a large factor.

Positron collisions with dust grains can be treated along the same lines as Zurek (1985) and Guessoum, Ramaty and Lingenfelter (1991) did, namely that the cross section is essentially a geometric one (πa^2) with the electric charge effect (attraction or repulsion with the positron depending on the local conditions) and the positron escape (backscattering and re-emission from the dust grain) taken into account:

$$\sigma_{gr} = (1 - R_+) \pi a^2 f_{elec}, \quad (2)$$

where a is the radius of the grain and R_+ is the probability that the positron is either backscattered by the grain or re-emitted after being captured. f_{elec} is given by $(1 - Ze^2/akT)$ or $\exp(-Ze^2/akT)$ depending on whether the grain is negatively or positively charged, respectively; Z is the grain charge, and T is the temperature of the medium. Grains are expected to be negatively charged in the hot and ionized phases of the ISM and possibly positively charged in the cold and neutral phases (being slightly ionized themselves by the UV radiation of nearby

stars if applicable). It can be shown (Krugel 2003) that the electric potential of a grain is 2.5 kT/e , so that the quantity $Ze^2/akT = 2.5$ is independent of the temperature of the medium or the size of the grain.

The positrons that are captured will diffuse and thermalize quickly with the grain molecules; infra-red emission of the ISM dust shows that the temperature of the grains varies between 15 K and 100 K depending on the conditions of the ISM medium (15K in the coldest phases, and between 50 K and 100 K in the ionized and hot conditions). Once thermalized, the positrons in the grains will form a positronium atom, which will either readily be in the para-state or be formed in the ortho-state but undergo a “pick-off” annihilation reaction as a para-state (giving 2 photons) when the positron (bound in the Ps) “picks off” an electron from the surrounding valence electrons. Most of the positrons that diffuse inside the grain will reach the surface, the diffusion length being greater than the diameter of most of the grains, but upon reaching the surface the positron will be captured in a “surface state” and form Ps there or be ejected, if the “positron work function” of the material is negative, which is the case for our dust grains (Rosenberg, Howell & Fluss 1987). A fraction of the Ps atoms formed at or near the surface will also be ejected if the “Positronium work function” for the material is negative, which is also the case for our dust (Hodges & Stott 1973, Nieminen & Oliva 1980, Eldrup et al. 1985, Rice-Evans & Rao 1988, Puska & Nieminen 1994).

Aside from the backscattering probability measured and simulated for Si and a few other elements (Makinen et al. 1992), we have found no specific measurements of e^+ and Ps probabilities for the materials that constitute our dust grains in the conditions that we deal with (slow positrons, etc.). There are some experiments (and a few calculations) that deal with metals (Huttunen et al. 1990; Nieminen & Oliva 1990) and polymers (Mukherjee, Chakravorty and Nambissan 1998) or conduct studies (probing) of defects in semi-conductors by positrons (Britton, Hempel and Triftshauser 2001; van Veen et al. 2004), but none that consider materials of the dust type.

We have adopted the value of 10 % of positron backscattering probability obtained by Makinen et al. (1992) when they extrapolate to the lowest positron energies (less than 1 keV), a value that seems to apply for all the materials they investigated (including Si).

For the rest of the parameters, we can only use measurements for materials that have similar chemical behavior (positron and Positronium negative work functions), and the closest we could find were copper and aluminum. For instance, the probability of re-emission of positrons from copper varies linearly with T from 0 to 15 % between 0 and 150 K, the temperature of the metal, which we will take as the temperature of the dust, in our case. (Nieminen & Oliva’s theoretical treatment predicted that this probability would tend to zero at very low temperatures.) The probability of ejection of Ps from the surface of the grain is found to be very similar for Cu and Al, taking the following approximate values: 0 at 0 K, 5 % at

25 K, 9 % at 50 K, 14 % at 100 K, 17 % at 150 K and 20 % at 200 K.

If these measurements are used for our dust grains (whose temperature ranges between 15 and 100 K), it would imply that the bulk (65 to 80 %) of the positrons colliding with grains will annihilate inside (giving two photons), a small fraction (5 to 15 %) will form Ps, be ejected and annihilate outside (giving two/three photons in the usual 25/75 % proportions), while 15 to 20 % of the positrons will simply fly back out after hitting a grain.

Figure 4 gives a schematic description of the main processes that a positron can undergo during its interaction(s) with dust grains.

The rate $r_{gr}(a)$ of positron capture by grains of size a is obtained from the effective cross section of positron capture by grains and the thermal speed of positrons in the medium:

$$r_{gr}(a) = n_{gr} \sigma_{gr} v_{e^+}, \quad (3)$$

where n_{gr} is the number density of dust grains in the ISM, σ_{gr} is the cross section of positron-capture by grains (Equation 2, and v_{e^+} is the average thermal speed of positrons in the given ISM phase: $v_{e^+} = \sqrt{\frac{3kT}{m_e}}$). n_{gr} is obtained from the overall mass of dust in the galaxy (0.6 % of the total gass mass) as well as the the grain size distribution $dN_{gr} = C_0 a^{-3/2} da$, which yields the mean value of the grain’s mass ($\langle m_{gr} \rangle_a = \int_{a_-}^{a_+} \rho_{gr} 4\pi/3 a^3 dN_{gr}$). The constant C_0 is inferred from the normalization condition $\int dN_{gr} = 1$. For the carbonaceous dust, the density is $\rho_{gr,C} \approx 2.24 \text{ g cm}^{-3}$; for the silicate dust, $\rho_{gr,Si/Mg/Fe} \approx 3.5 \text{ g cm}^{-3}$. A simple calculation, assuming the total dust mass to be equally divided into the two main types, then gives: $n_{gr} \approx 3.5 \times 10^{-13} n_H$ for the carbonaceous dust and $1.8 \times 10^{-12} n_H$ for the silicate dust.

Replacing σ_{gr} by its expression (Equation 2) in Equation 3 allows one to show explicitly the factors that influence the value of the positron capture rate: the reflection factor R_+ of positrons backscattered or ejected from the dust grain as explained above, the electrostatic enhancement of inhibition of positron-grain collision f_{elec} . We add an additional factor f_{dest} to take into account the potential destruction of dust grains, most likely in the hot environments. Averaging over the grain size distribution, the rate then becomes:

$$r_{gr} = n_{gr} (1 - R_+) f_{elec} f_{dest} \langle \sigma_{gr,geom} \rangle_a v_{e^+}, \quad (4)$$

where $\sigma_{gr,geom} = \pi a^2$ is the geometric cross-section and $\langle \sigma_{gr,geom} \rangle_a$ the mean value of the geometric cross section. As stated previously, dust is likely to be partially destroyed only in the hot phase of the ISM, so we take $f_{dest} = 0.5$ in that case, and $f_{dest} = 1$ in all other conditions. In the hot and warm-ionized phases, grains are widely considered to be negatively charged, with a potential such that $Ze^2/akT \approx -2.5$, so that $f_{elec} = 1 - Ze^2/akT \approx 3.5$; in the cold and neutral phases, however, the grains are assumed to be positively charged, but their electrostaic po-

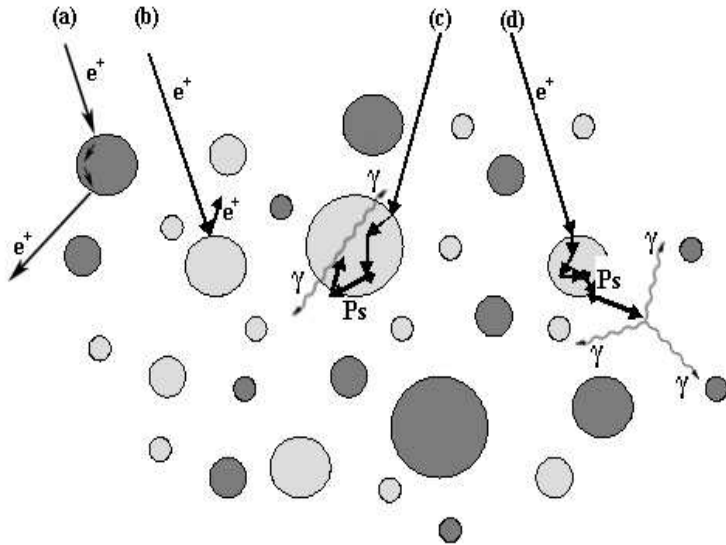


Fig. 4. Collisions and subsequent annihilation of positrons with grains (of various sizes and types) - (a) positron re-emission, (b) positron backscattering, (c) Positronium in grain, (d) Positronium ejection.

tential depends on local conditions (proximity of an ionizing UV radiation from a neighboring hot star, etc.), so that the potential can vary between 0 and 2.5 V; in these cases, and considering the de facto impossibility of pinpointing such a value we take $f_{elec} = \exp(-Ze^2/akT) \approx 0.5$, keeping in mind that such a factor is in effect irrelevant in the cold phase since the dust has no effect on the annihilation there.

Taking all these factors into account then yields final values for the positron capture rates by the carbonaceous and the silicate dust for the various ISM phase conditions, as reported in Table 3.

The rates obtained and reported here are in most cases essentially the same as those of Guessoum, Ramaty and Lingenfelter (1991), but in some cases and due to the use of new data, the rates are substantially different. The differences are found in the rates of charge exchange with H in the warm neutral phase, where our new value is greater than the previous one by about 33 %; direct annihilation with H in the warm neutral phase, where our rate is greater than the old one by about 16 %; capture by grains, where our rates are about a factor of 10 lower, a factor of 3 lower and a factor of 1.5 greater than the old values in the cold, warm neutral and hot phases respectively.

The width of the annihilation line resulting from the decay of the Ps produced inside the grain is an important quantity. There are actually two widths, corresponding to the annihilation of the Ps atoms that escape and those that remain and die in the grains. Nieminen & Oliva (1980) state that the kinetic energy of the Ps ejected by the grain is equal to the absolute value of the “Ps work function” ϕ_{Ps} of the material. This implies a width $\Gamma_{gr,out} = 2\sqrt{m_e c^2 \phi_{Ps}}$ of about 1.4 keV, taking $\phi_{Ps} \approx 1$ eV. (Note that the value used for $\Gamma_{gr,out}$ since Guessoum,

Ramaty and Lingenfelter 1991 was 2.5 keV. Moreover, the fraction of Ps escaping from the grain is now taken to be 5 - 15 %, compared to the previously held 1/3 value. This will have some significant impact on the shape of the annihilation line, at least in the hot and ionized phases.) The width of the line produced by para-Ps decaying inside the grain cannot be estimated via other physical quantities and needs to be measured in the laboratory. Again, there have been no measurements for the kinds of materials that make up our grains, but typical ACAR (angular correlation of the annihilation radiation) measurements of the two emitted photons give values $\theta_{ACAR} 5-8$ mrad (Biasini et al. 2000; Sasaki et al. 2003), which would translate into $\Gamma_{gr,in} = 0.5\theta_{ACAR} m_e c^2 \approx 1.3 - 2.0$ keV. We note, however, that the measurements of $\Gamma_{gr,in}$ by Iwata, Greaves and Surko (1997) for many atoms and molecules (including complex alcohols) shows the width to be always between 2.0 keV and 3.0 keV. We have thus adopted the higher value of the ACAR measurements, which corresponds to the lowest value of the annihilation on molecules: $\Gamma_{gr,in} \approx 2.0$ keV.

4. Annihilation spectra

Having reviewed and recalculated the various processes' reaction rates and line widths, we can construct the standard spectra of the annihilation radiation for each phase of the ISM as well as an overall “global” or “diffuse” radiation spectrum, one that includes contributions from the various regions; the latter “global” spectrum requires knowledge about the relative distribution of the ISM phases and their volume contributions to the emitted radiation.

Table 3. Reaction rates (in cm³/s) for the various processes after thermalization in the different ISM phases.

Process / Medium	Molecular (T ≈ 10 K)	Cold (T ≈ 80 K)	Warm Neutral (T ~ 8000 K)	Warm Ionized (T ~ 8000 K)	Hot (T ~ 10 ⁶ K)
Charge Exchange with H	--	--	1.8 × 10 ⁻¹²	--	--
Charge Exchange with H ₂	--	--	--	--	--
Charge Exchange with He	--	--	9.0 × 10 ⁻²¹	9.0 × 10 ⁻²¹	--
Direct Annihilation with H	--	6.5 × 10 ⁻¹⁴	4.4 × 10 ⁻¹⁴	--	--
Direct Annihilation with H ₂	4.3 × 10 ⁻¹³	--	--	--	--
Direct Annihilation with He	1.5 × 10 ⁻¹³	3.7 × 10 ⁻¹⁴	2.6 × 10 ⁻¹⁴	2.6 × 10 ⁻¹⁴	--
Radiative Combination	--	--	--	1.2 × 10 ⁻¹²	1.3 × 10 ⁻¹⁴
Direct Annihilation with electrons	--	--	--	1.7 × 10 ⁻¹³	1.8 × 10 ⁻¹⁴
Capture by grains	2.4 × 10 ⁻¹⁶	6.8 × 10 ⁻¹⁶	6.5 × 10 ⁻¹⁵	4.6 × 10 ⁻¹⁴	2.4 × 10 ⁻¹³

The emission processes are spectroscopically modeled as either a pure two-photon direct annihilation represented by a Gaussian with a given FWHM or a combined two-photon-line/three-photon-continuum when the annihilation proceeds via formation of a positronium atom; in this latter case, the two-photon line is represented by a Gaussian with its characteristic FWHM, while the continuum part is represented by the usual Ore & Powell (1949) function $P_t(E)$ that describes the probability of the emitted photon being emitted with an energy E between 0 and 511 keV (Eq. 10 of Guessoum, Ramaty and Lingenfelter, 1991).

Table 4 summarizes the line widths for various processes. For several processes the Gaussian function with a given FWHM represents a slight simplification of the real spectrum, but the annihilation spectra obtained in the end, and their eventual comparison with the data, are insensitive to this level of precision.

However, several values of the various processes' FWHM have now changed to some extent (by about 10 % in most cases, but sometimes more) compared to the values used in previous modeling. In particular, the width of the line produced in the decay of Ps formed “in-flight” with H is now 5.8 keV instead of the 6.4 keV used for over two decades. (The difference is due to the accurate experimental cross sections now available for positron excitation, ionization and charge exchange with H.) Likewise the lines resulting from positron annihilation after capture by a grain (either two-photon annihilation inside the grain or decay of the Ps ejected from the grain) have widths of 2.0 keV and 1.4 keV respectively, compared to 1.8 keV and 2.5 keV previously. References and discussions of the various FWHMs are given in the sections 3.2 and 3.3.

The following formula then allows us to construct the theoretical spectrum for a given ISM phase:

$$S(E) = \int dE' \left[3 \times \frac{3}{4} P_t(E') + 2 \times \frac{1}{4} \delta(E' - E_0) \right] \\ \{ X \times f_{1,H/H_2} G(E, E', \Gamma_{if,H/H_2}) \\ + Y \times f_{1,He} G(E, E', \Gamma_{if,He}) \\ + (1 - X f_{1,H/H_2} - Y f_{1,He}) \right]$$

$$\times [f_{ce,H/H_2} G(E, E', \Gamma_{ce,H/H_2}) \\ + f_{ce,He} G(E, E', \Gamma_{ce,He}) \\ + f_{rce} G(E, E', \Gamma_{rce}) \\ + f_{gr,out} G(E, E', \Gamma_{gr,out})] \} \\ + 2 (1 - X f_{1,H/H_2} - Y f_{1,He}) [f_{dae} G(E, E_0, \Gamma_{dae}) \\ + f_{da,H/H_2} G(E, E_0, \Gamma_{da,H/H_2}) \\ + f_{da,He} G(E, E_0, \Gamma_{da,He}) \\ + f_{gr,in} G(E, E_0, \Gamma_{gr,in})] , \quad (5)$$

where X and Y are the relative abundances of H/H₂ and He (90 % and 10% respectively), Γ_P refers to the FWHM of the line produced by a given process P (if, ce, dae, daH, gr refer to in-flight, charge exchange, direct annihilation with free electrons, direct annihilation with H, annihilation with grains – inside or outside –, etc.); $G(E, E', \Gamma_P)$ is the Gaussian function of variable E', centered on E, and of FWHM = Γ_P , normalized to 1; the factors f_P are the relative probabilities for each process: $f_P = R_P / \sum R_P$, R_P denoting the rates of various processes (Table 3) weighted by the relative abundance of each element.

Figures 5 (a, b, c, d, e) show the annihilation spectrum in the molecular, cold (atomic), warm neutral, warm ionized and hot phases, respectively. In each case the solid curve shows the spectrum assuming a “standard grain model” (in terms of grain abundance, size distribution, composition, etc., as adopted in Section 3.3) in the given phase, i.e. a factor $x_{gr} = 1$; dashed curves represent the spectra in the case of grains greatly amenable to positron capture ($x_{gr} = 10.0$); dotted curves represent the spectra when dust is removed from the phase. The spectra confirm that unless dust is overabundant in the warm ionized or hot phases (or the rates of capture are greater than we have adopted – as explained in section 3.3), it has a negligible effect on the annihilation radiation emitted in the ISM.

In order to construct the “global” spectrum of 511 keV annihilation from the ISM as a whole, one simple approach is to combine the previous phase spectra on the basis of the relative contributions (densities and filling factors) of each phase. For this, filling factors such as those used in the ISM model of McKee & Ostriker (1977) can be adopted:

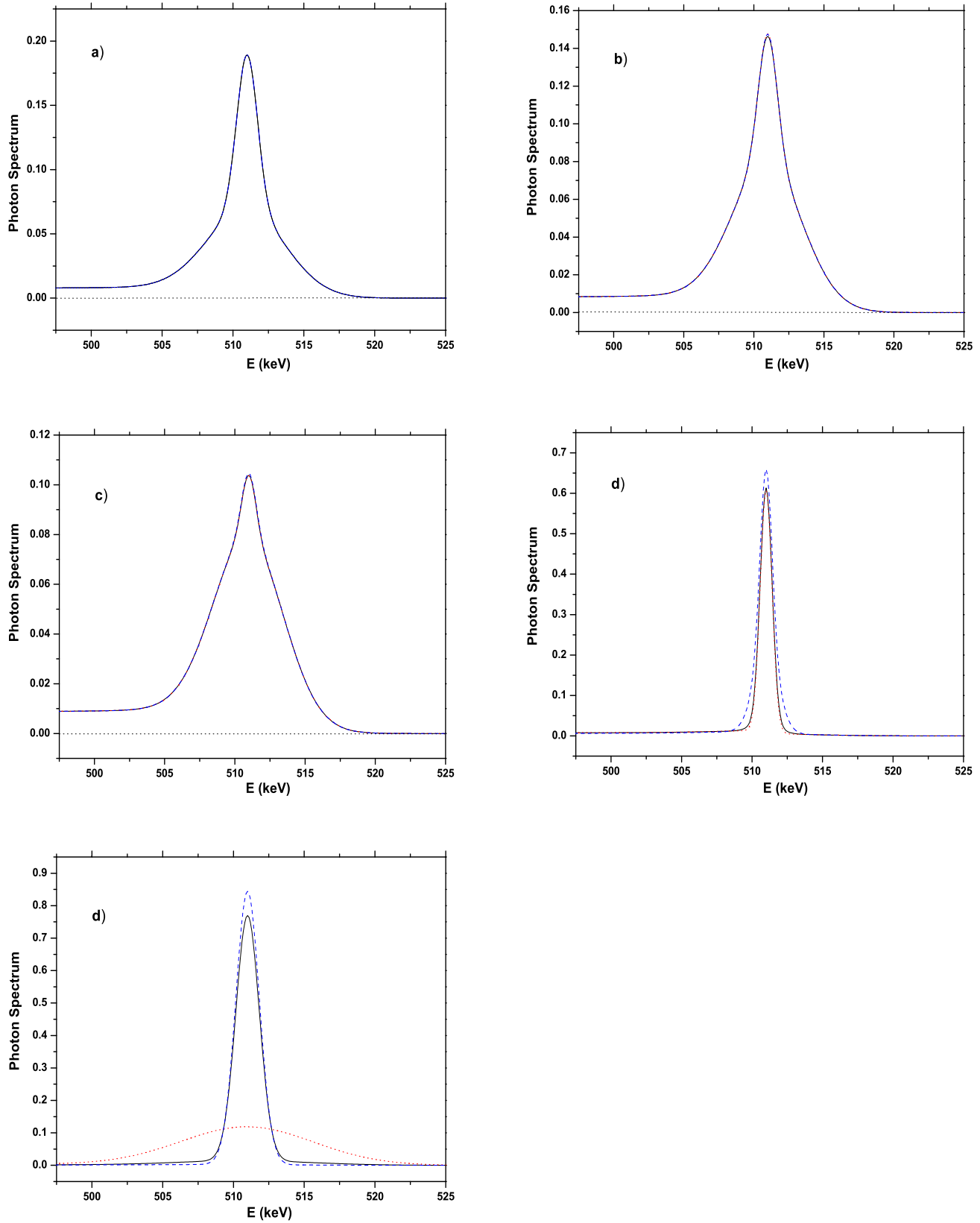


Fig. 5. Annihilation spectra for the 5 ISM phases separately (see text): (a) Cold, molecular hydrogen medium; (b) Cold, atomic hydrogen medium; (c) Warm, neutral medium; (d) Warm, ionized medium; (e) hot medium.

Table 4. Line widths (in keV) for various positron annihilation processes.

Process / Medium	Cold & Molecular (T < 100 K)	Warm Neutral (T ~ 8000 K)	Warm Ionized (T ~ 8000 K)	Hot (T ~ 10 ⁶ K)
Charge Exchange with H in-flight	5.8	5.8	--	--
Charge Exchange with H ₂ in-flight	6.4	--	--	--
Charge Exchange with He in-flight	7.4	7.4	8.7	--
Charge Exchange with H after thermalization	--	1.16	--	--
Charge Exchange with H ₂ after thermalization	--	--	--	--
Charge Exchange with He after thermalization	--	1.22	1.22	--
Direct Annihilation with H	1.56	1.56	--	--
Direct Annihilation with H ₂	1.71	--	--	--
Direct Annihilation with He	2.50	2.50	2.50	--
Radiative Combination	--	--	0.98	11
Direct Annihilation with electrons	--	--	0.98	11
Positronium from grains	1.4	1.4	1.4	1.4
Annihilation in grains	2.0	2.0	2.0	2.0

2.4 % for the cold phase(s), 23 % for each of the warm phases and 52% for the hot phase. In the same model, the densities of each phase are: 42 cm⁻³, 0.37 cm⁻³, 0.25 cm⁻³, 3.5 × 10⁻³ cm⁻³ in the cold, warm neutral, warm ionized and hot phases, respectively.

Figure 6 shows the result of combining the individual-phase spectra using the McKee & Ostriker simple prescription as well as the spectra obtained when the positrons are excluded from the cold regions (both the molecular and atomic phases); this we do for comparative purposes with the results obtained in the treatment of Guessoum, Ramaty and Lingenfelter (1991). In the first case (annihilation in all phases according to the description of McKee & Ostriker), we see that the dust makes no difference to the line profile. In the second case, the profile of the overall emission spectrum is substantially different from the “uniform” case, and the dust does make a non-negligible difference.

A more physically realistic approach would be to adopt an analytic ISM model such as Ferriere’s, which gives the densities of each species (H, H₂, free electrons, etc.) in each volume element (defined by its galactocentric coordinates r and z) of the ISM. This latter approach we save for a future, more physical treatment of annihilation in the ISM, one that will consider the change in the annihilation spectrum and profile when emanating from different directions and regions of the Galaxy.

Table 5 displays the FWHMs of the lines obtained in each phase as well as in the “global” case. These allow us to compare our results with earlier ones and serve to give us a rough idea about the physical properties of the annihilation region(s), although we must emphasize that the FWHM parameter is not a sufficient parameter in characterize such spectra. Until the full follow-up modeling and interpretation work is performed, these values are used for comparison and indication purposes. Our present results are largely consistent with the older ones, but our line widths tend to be slightly larger than the older ones in all phases. In the warm neutral phase the line appears

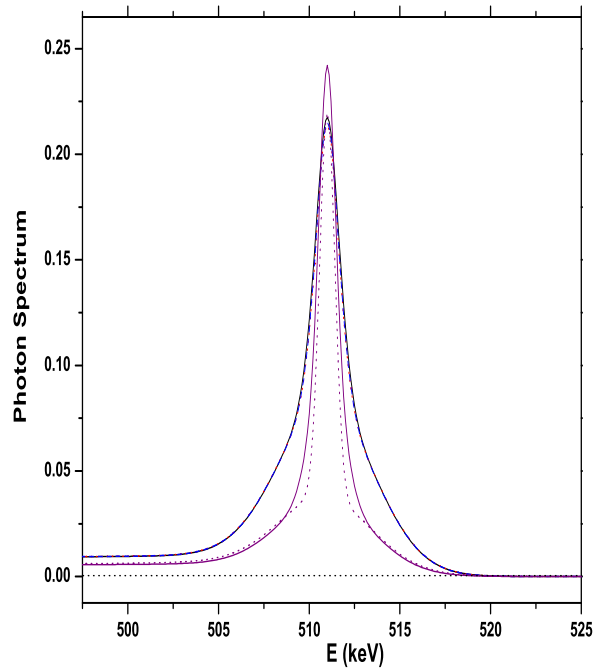


Fig. 6. Combined (“global”) ISM annihilation spectra, obtained under two assumptions: 1) positrons annihilating in all phases according to the filling factors and densities given in the McKee & Ostriker (1977) model, either with or without the effect of the grains (solid, blue dashed and red dotted curves); 2) positrons not annihilating in the cold phases, with/without grain effect (solid and dotted narrower purple curves).

to be substantially broader than the result of Guessoum, Ramaty and Lingenfelter (1991), but only because in that treatment the warm neutral phase has a 15 % ionization fraction, whereas in the present treatment the warm neutral phase is completely neutral. Moreover the rate for

Table 5. Values of FWHMs obtained (in keV) in each ISM phase separately and in the “global” case; the values are given for the “standard grain model” ($x_{gr} = 1$), for $x_{gr} = 0$ (no dust) and for $x_{gr} = 10$ (overabundant and/or grain characteristics especially favorable for positron capture – see text), respectively. For the “global (combined)” spectrum we give FWHM values in two cases: the McKee & Ostriker model with its phase densities and filling fractions, and the situation (results in parentheses) when the positrons are excluded from the cold phases.

Phase	$x_{gr} = 1$	$x_{gr} = 0$	$x_{gr} = 10$
Molecular	2.39	2.39	2.39
Cold	3.00	3.00	2.92
Warm Neutral	4.78	4.76	4.74
Warm Ionized	1.02	1.00	1.19
Hot	1.99	11.0	1.96
Combined	2.26 (1.18)	2.17 (1.15)	2.17 (1.37)

charge exchange with H has increased (by about 20 %) in this work, which increases the contribution of the broad line; indeed the in-flight process, for which the line widths are always large (≈ 6 keV), has now become more dominant overall.

The main conclusions from this “phase” treatment are first that the “global” spectra obtained here (on the basis of the McKee & Ostriker 1977 ISM model) are consistent with the observed widths reported by the various missions (including SPI and TGRS) and second that unless specific physical assumptions are made regarding whether the positrons annihilate preferentially in some regions (say the hot and/or ionized phases), the dust will in general play a negligible role. A careful analysis and interpretation of the observational data in the light of our new modelling of the positron processes will be performed in a follow-up work, and we do not exclude a priori the possibility that positrons may show a preference for some phases and/or for grain capture.

5. Summary and conclusions

The aim of this work was to carefully reexamine all the processes that positrons undergo in the ISM, including the complicated interactions with dust grains, and to try to determine as precisely as possible all the quantitative factors in the problem, particularly the various reaction rates and the widths of the lines emitted in the process. We also included all aspects of positron interactions with molecular hydrogen, in addition to atomic hydrogen, as well as helium (excitation, ionization, charge exchange, direct annihilation with the bound electron, etc.). For this we undertook a major review of the literature (cross section measurements and calculations, etc.) and performed a detailed Monte Carlo simulation that allowed us to obtain new, accurate results on the fraction of positrons that form positronium in flight, the profile and width of the

line emitted in the process, the lifetimes of the positrons in such conditions, etc. We also investigated in detail the interstellar dust and its effect on positron annihilation. The final results of our calculations (reaction rates and spectra) showed that dust is only important in the hot phase of the ISM (where it dominates all other processes), but previous modelling efforts (e.g. Guessoum et al. 2004) stressed the importance of this process. There are still some pieces of the puzzle missing in this regard, for example the widths of the lines emitted in the annihilation of positrons/positroniums inside/outside a dust grain, the extent of the destruction of grains in the hot/warm regions of the ISM and also the electrostatic charge carried by dust in various conditions.

We aimed to provide solid basis for modelling the detailed annihilation data currently being obtained by INTEGRAL-SPI (Knodlseder et al. 2005) as well as future observations, e.g. spectroscopic explorations of regions of the Galaxy other than the central regions (galactic plane, compact objects / LMXBs, etc.). Indeed, with the positron processes now much more firmly understood and quantified, it becomes possible to compare the annihilation model outlined here and the spectra obtained by our calculations with the SPI data and infer useful information regarding the regions where the annihilation is predominantly taking place. It will also become possible to model and interpret data obtained for more local and specific places. Finally, with the microscopic processes now fully examined and more precisely parametrized, it becomes possible to perform a time-dependent investigation of the lives of positrons from their births to their ultimate deaths/annihilations. This would then constitute a major step towards the resolution of the “origin of positrons in the Galaxy” puzzle.

Acknowledgements. N. Guessoum would like to acknowledge the support of the INTEGRAL project. The researchers and staff of the Centre d’Etude Spatiale des Rayonnements (Toulouse, France) are thanked for their kind hospitality during the various times when much of this work was conducted. Cliff Surko is thanked for helpful discussions and for providing us with useful references.

References

- Armour, E.A.G., Baker, D.J. & Plummer, M., 1990, J. Phys. B, 23, 3057
- Berakdar, J. 1998, Phys. Rev. Letters, 81, 1393
- Bhatia, A. K., Drachman, R. J., and Temkin, A. 1977, Phys. Rev. A, 16, 1719
- Biasini, M. et al. 2000, J. Phys. Condens. Matter, 12, 5961
- Book, D.L. & Ali, A.W. 1975, NRL Memorandum Rept. 2898
- Britton, D. T., Hempel, A., Triftshauser, W. 2001, Phys. Rev. Letters, 87, 217401
- Brown, B. L. et al. 1984, Phys. Rev. Letters, 53, 2347
- Brown, B. L. & Leventhal, M., 1986, Phys. Rev. Letters, 57, 1651
- Brown, B. L., Leventhal, M., and Mills, A. P., Jr. 1986, Phys. Rev. A, 33, 2281

Bussard, R. W., Ramaty, R., and Drachman, R. J. 1979, *ApJ* 228, 928

Campbell, C.P. et al. 1998, *Nuc. Inst. Meth. B*, 143, 41

Campeanu, R. I. & Humberston, J. W., 1977, *J. Phys. B Letters*, 10, 153

Chapuis, C. et al., 1991; *Gamma-Ray Line Astrophysics; Proceedings of the International Symposium*, Paris, France, Dec. 10-13, 1990. New York: American Institute of Physics (AIP), 1991. Edited by Philippe Durouchoux and Nikos Prantzos. AIP Conference Proceedings, Vol. 232., p.54

Chapuis, C. et al., 1994, *ApJ Supp.*, 92, 545

Charlton, M. et al. 1988, *J. Phys. B Letters*, 21, 545

Charlton, M. & Humberston, J. W. 2001, "Positron Physics", Cambridge University Press,

Chen, X.X., Chen, J. & Kuang, J., 1992, *J. Phys. B Letters*, 25, 5489

Coleman, P. G. et al. 1982, *Can. J. Phys.*, 60, 584

Crannell, C. J. et al. 1976, *ApJ* 210, 582

Dannefaer, S. et al. 1996, *J. Appl. Phys.*, 79, 12

Dermer, C. D. & Murphy, R. J. (2001) In: *Exploring the gamma-ray universe. Proceedings of the Fourth INTEGRAL Workshop*, 4-8 September 2000, Alicante, Spain. Editor: B. Battrick, Scientific editors: A. Gimenez, V. Reglero & C. Winkler. ESA SP-459, Noordwijk: ESA Publications Division, ISBN 92-9092-677-5, 2001, p. 115

Diana, L. M. et al. 1986, *Phys. Rev. A*, 34, 2731

Draine, B. T. 2003, *Ann. Rev. A & A*, 41, 241

Draine, B. T. 2004, *Carnegie Observatories Astrophysics Series*, Ed. A. McWilliam & M. Rauch, 320.

Dupasquier, A. & Mills, A. P. Jr. (editors) 1995, *Positrons Solid-State Physics*, Proc. Internat. School of Physics "Enrico Fermi", Course CXXV, Varenna 1993, IOS Press, Amsterdam.

Durouchoux, P. et al. 1993, *A & A Supp.*, 97, 185

Eldrup, M. et al. 1985, *Phys. Rev. B*, 32, 7048

Ferriere, K. 1998a, *ApJ*, 497, 759

Ferriere, K. 1998b, *ApJ*, 503, 700

Ferriere, K. M. 2001, *Rev. Mod. Phys.*, 73, 1031

Ferriere, K. M. 2003, in "Physique et Astrophysique du Rayonnement Cosmique", Proceedings of Ecole de Goutelas held 2-6 June 2003, Goutelas, France, Edited by E. Parizot, A. Marcowith, V. Tatischeff, G. Pelletier & P. Salati, Observatoire Astronomique de Strasbourg & SF2A, p. 7

Ficocelli Varrachio E. & Parcell, L.A. 1992, *J. Phys. B*, 25, 3037

Fornari, L.S., Diana, L.M. & Coleman, P.G. 1983, *Phys. Rev. A*, 51, 2276

Fromme, D. et al. 1986, *Phys. Rev. Letters*, 57, 3031

Fromme, D. et al. 1988, *J. Phys. B*, 21, 262

Gehrels, N. et al., 1991, *ApJ Letters*, 375, 13

Goruganthu, R.R. et al. 1985, *Phys. Rev. A.*, 34, 103

Gould, R. J. 1989, *ApJ*, 344, 232

Guessoum, N., Ramaty, R., and Lingenfelter, R. E. 1991, *ApJ*, 378, 170

Guessoum, N., Ramaty, R., and Skibo, J. G. 1997, in "The Transparent Universe," Proceedings of the 2nd INTEGRAL Workshop held 16-20 September 1996, St. Malo, France, Edited by C. Winkler, T. J.-L. Courvoisier, and Ph. Durouchoux, European Space Agency, 1997, p.113

Guessoum, N. et al. 2004, in "The Integral Universe," Proceedings of the 5th INTEGRAL Workshop held 16-20 February 2004, Munich, Germany, in press.

Harris, M. J. et al. 1998, *ApJ Letters*, 501, 55

Harris, M. J. et al. 2000, *The Fifth Compton Symposium, Proceedings of the fifth Compton Symposium*, held in Portsmouth, NH, USA, September 1999. Melville, NY: American Institute of Physics (AIP), 2000. Edited by Mark L. McConnell and James M. Ryan AIP Conference Proceedings, Vol. 510., p.31

Heitler, W. 1954, *Quantum theory of radiation, International Series of Monographs on Physics*, Oxford: Clarendon, 1954, 3rd ed.

Herter, T. et al. 1989, *ApJ*, 343, 696

Hewitt, R. N., Noble, C. J., & Bransden, B. H., 1992, *J. Phys. B*, 25, 2683

Hodges, C.H. & Stott, M.J., 1973, *Phys. Rev. B*, 7, 73

Hofmann et al. 1997, *J. Phys. B.*, 30, 3297

Huttunen, P. A. et al. 1990, *Phys. Rev. B*, 42, 1560

Iwata, K., Greaves, R. G., and Surko, C. M. 1996, *Can J. Phys.*, 74, 407

Iwata, K., Greaves, R. G., and Surko, C. M. 1997, *Phys Rev A*, 55, 3586

Iwata, K. et al. 1997, *Phys. Rev. Letters*, 79, 39

Iwata, K. et al. 2000, *Phys. Rev. A*, 61, 2719

Jacobsen et al. 1995, *J. Phys. B.*, 28, 4691

Janev, R.K. & Solov'ev, E.A. 1998, *J. Phys. B*, 32, 3215

Jean, P. et al. 2004, in "The Integral Universe," Proceedings of the 5th INTEGRAL Workshop held 16-20 February 2004, Munich, Germany, in press.

Johnson, W. N., Harnden, F. R., and Haymes, R. C., 1972, *ApJ*, 172, 1

Jones, G.O. et al. 1993, *J. Phys. B*, 26, 483

Kara, V. 1999, PhD Thesis, University of London

Kernoghan, A. A. et al. 1996, *J. Phys. B*, 29, 2089

Köver, A. & Laricchia, G. 1998, *Phys. Rev. Letters*, 80, 5309

Köver, A., Paludan, K., & Laricchia, G. 2002, *Nucl. Inst. Meth. B*, 192, 167

Knodlseder, J. et al. 2004, *A & A*, in preparation

Knudsen, H. et al. 1990, *J. Phys. B*, 23, 3955

Krugel, E. 2003, "The Physics of Interstellar Dust", The Institute of Physics, London

Kwan, C.K. et al. 1998, *Nucl. Inst. Meth. B*, 143, 61

Leventhal, M. 1973, *ApJ Letters*, 183, 147

Leventhal, M., MacCallum, C. J., Stang, P. D. 1978, *ApJ Letters*, 225, 11

Leventhal, M. et al. 1993, *ApJ Letters*, 405, 25

Li, A. 2004, "Astrophysics of Dust", Witt, A. N., Clayton, C., & Draine, B. T., ASP Conference Series, vol. 309

Li, A. & Draine, B. T. 2001, *ApJ*, 554, 778

Lonjou, V. et al. 2004, in "The Integral Universe," Proceedings of the 5th INTEGRAL Workshop held 16-20 February 2004, Munich, Germany, in press.

Makinen, J. et al. 1992, *JPCM Lett*, 4, 503

McAlinden, M.T & Walters, H.R.J. 1992, *Hyperfine Interactions*, 73, 65

McKee, C. F. & Ostriker, J. P. 1977, *ApJ*, 218, 148

Mills, A. P. et al. 1989, *Phys. Rev. B*, 40, 8616

Milne, P. A. et al. 2000, *American Astronomical Society, HEAD Meeting #5, #40.06*; *Bulletin of the American Astronomical Society*, Vol. 32, p.1253

Mokrushin, A. et al. 2003, *Phys. Stat. Sol.*, 197, 212

Mori, S. & Suoeka, O. 1994, *J. Phys. B.*, 17, 3295

Moxom, J. et al. 1993, *J. Phys. B*, 26, 367

Moxom, J., Ashley, P., & Laricchia, G. 1996, *Can. J. Phys.*, 74, 367

Mukherjee, M., Chakravorty, D., Nambissan, P. M. G. 1998,
 Phys. Rev. B, 57, 848

Niemenen, R. M. & Oliva, J. 1980, Phys. Rev. B, 22, 2226

Omidvar, K. 1965, Phys. Rev., 140, 38

Ore, A. & Powell, J. L. 1949, Phys. Rev., 75, 1963

Overton, N., Mills, R. J., Coleman, P. G., 1993, J. Phys. B, 26,
 3951

Parcell, L.A. et al. 1987, J. Phys. B, 20, 2307

Paul, J. 2004, Nuc. Inst. Meth. B, 221, 215

Pi, X. D. et al. 2003, Physica B, 340-342, 1094

Purcell, W. R. et al. 1997, ApJ, 491, 725

Puska, M. J., Niemenen, R. M. 1994, Rev. Mod. Phys., 66, 841

Ramaty, R. & Meszaros, P. 1981, ApJ, 25, 384

Rapp, D., Englander-Golden, P. & Briglia, D.D 1965, J. Chem.
 Phys., 42, 4081

Ratnavelu, K. 1991, Au. J. Phys., 44, 265

Rice-Evans, P. & Rao, K.U. 1988, Phys. Rev. Letters, 61, 581

Rosenberg, I.J., Howell, R.H. & Fluss, M.J. 1987, Phys. Rev.
 B, 35, 2083

Sasaki et al. 2003, Radiation Physics and Chemistry, 68, p.
 569-572

Sperber, W. et al. 1992, Phys. Rev. Letters, 68, 3690

Spicher, G. et al. 1990, Phys. Rev. Letters, 64, 1019

Stecker, F. W. 1969, Ap& S S, 3, 579

Steigman, G. 1968, Ph.D. Thesis – New York University.
 Source: Dissertation Abstracts International, Volume: 30-
 01, Section: B, page: 0324

Stein, T.S. et al. 1998, Nuc. Inst. Meth. B, 143, 68

Surko, C. M. et al. 2000, Nuc. Inst. Meth. B, 171, 2

Suzuki, R. et al. 2003, Rad. Phys. & Chem., 68, 339

Teegarden, B. J. et al., 1996, ApJ Letters, 463, 75

van Veen, A. et al. 2004, Materials Science Forum, 445-446,
 254

Wallyn, P. et al. 1993, ApJ, 403, 621

Wallyn, P. et al. 1994, ApJ, 422, 610

Walters, H.R.J. 1988, J. Phys. B, 21, 1893

Weber, M. H. & Lynn, K. G. 2000, Rad. Phys. & Chem., 58,
 2000

Weingartner, J. C. & Draine, B. T. 2001, ApJ, 548, 296

Weiss, A. H. et al. 1994, Radiation Physics and Chemistry, 44,
 665

Zhou, S. et al. 1997, Phys. Rev. A, 55, 361

Zurek, W. H. 1985, ApJ, 289, 603